Proceedings of the
International Meteor Conference
La Palma, Canary Islands, Spain
20–23 September, 2012

Meteor shower flux densities and the zenith exponent

Sirko Molau[1] and Geert Barentsen[2]

[1] **Arbeitskreis Meteore e.V., Abenstalstr. 13b, D-84072 Seysdorf, Germany**
sirko@molau.de

[2] **University of Hertfordshire, United Kingdom**
geert@barentsen.be

The METREC software was recently extended to measure the limiting magnitude in real-time, and to determine meteor shower flux densities. This paper gives a short overview of the applied algorithms. We introduce the METREC FLUX VIEWER, a web tool to visualize activity profiles on-line. Starting from the Lyrids 2011, high-quality flux density profiles were derived from IMO Video Network observations for every major meteor shower. They are often in good agreement with visual data. Analyzing the 2011 Perseids, we found systematic daily variations in the flux density profile, which can be attributed to a zenith exponent $\gamma > 1.0$. We analyzed a number of meteor showers in detail and found zenith exponent variations from shower to shower in the range between 1.55 and 2.0. The average value over all analyzed showers is $\gamma = 1.75$. In order to determine the zenith exponent precisely, the observations must cover a large altitude range (at least 45°).

1 Introduction

The IMO Video Meteor Network has been developing prosperously in the previous few years. The number of observers and cameras grew continuously, and so has the effective observing time and number of meteors collected each year. By the end of 2011, 46 observers from 16 countries (mainly in central Europe) operated an overall of 80 video cameras (Molau et al., 2012c). During 2011, the IMO Video Meteor Database had grown to over one million meteors (Molau et al., 2012b).

Unlike for other video networks, the focus of the IMO Video Meteor Network is on single-station observations, as this gives no limitation for the location of the observers. No matter where in the world you are observing and how many cameras there are in your vicinity—your video meteor observations are a valuable input to the IMO Video Meteor Network. One reason is, that we do not (only) focus on radiants and orbits. In particular, the activity profile and interval of meteor showers have been analyzed by us recently.

2 Limiting magnitude, effective collection area, and flux densities

The METREC software, which is used by all members of the IMO Video Meteor Network, was been completed and extended over many years. Recently, it was extended with the functionality to measure the limiting magnitude on-line during the observation (Molau, 2010). The procedure consists of five basic steps (see Figure 1):

1. from the video stream, a mean background image is calculated;

2. with a high-pass filter, stars are segmented in the mean background image;

3. a star map is calculated from the inverse plate constants and the observing date and time. It shows which star is currently expected at what position;

4. the segmented stars are identified by matching them against the star map; and, finally,

5. the limiting magnitude is derived from the total number of identified stars. This step is identical to the star field counting in visual observations.

METREC is executing these steps in real-time, and the limiting magnitude is determined and stored every minute. Limiting-magnitude determination is the key to measure flux densities, but it is also the most critical step of the analysis. It is steered by three parameters (Molau et al., 2011c):

1. the noise level that defines how much brighter than the background a star must be to be segmented;

2. the limiting magnitude for the star map; and

3. the maximum accepted spatial distance between a segmented star and a star from the star map.

Thanks to the dynamical adjustment of the first two parameters, the calculation of the limiting magnitude is quite robust for a wide range of meteor cameras with different characteristics. Still, further improvements are continuously implemented.

Once the limiting magnitude is measured, METREC can calculate the effective collection area of a video system. The procedure is as follows (Molau, 2010):

1. the angular extent (in square degrees) is calculated of each pixel by determining the equatorial coordinates of the pixel boundaries;
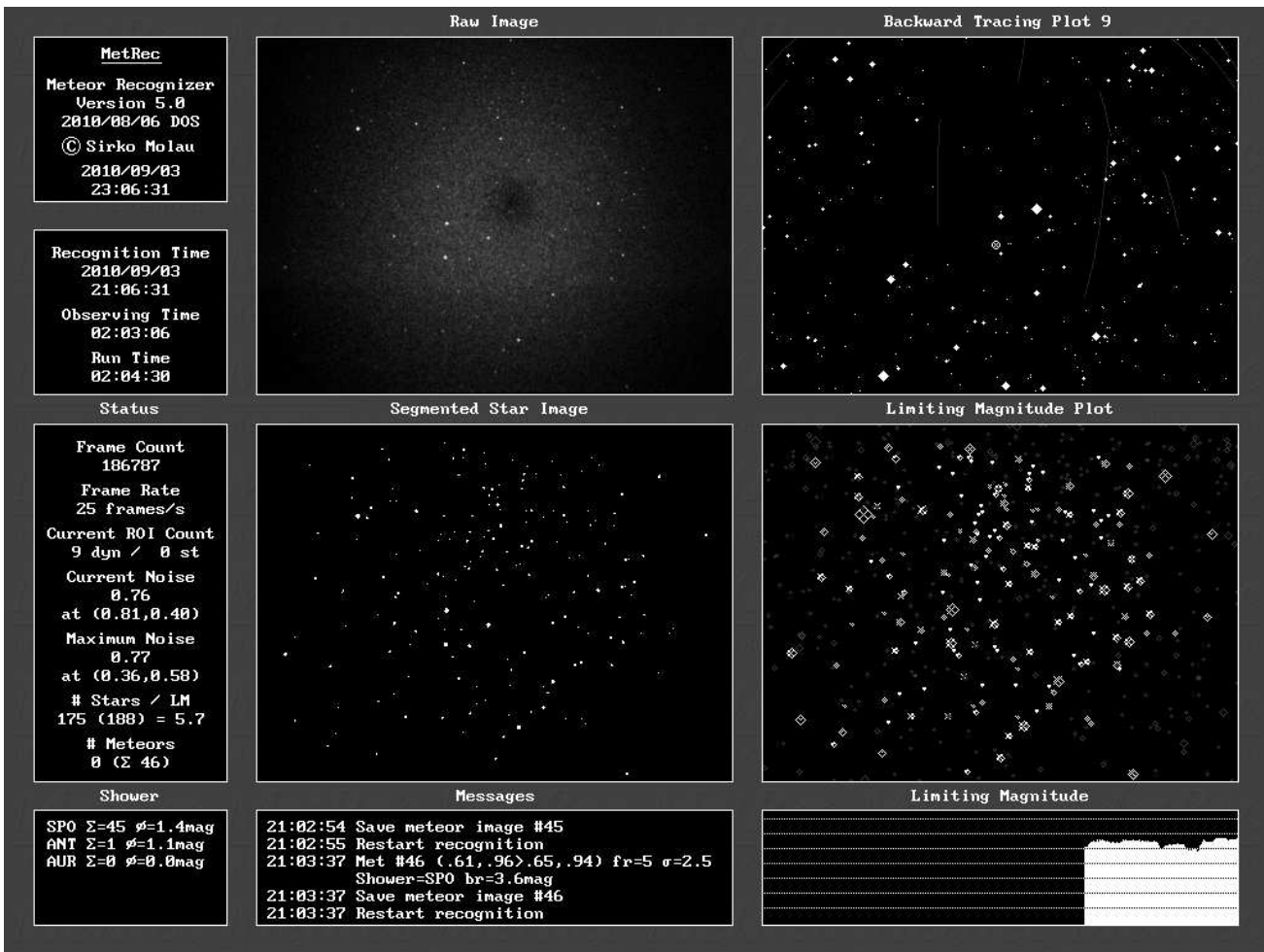
Figure 1 – The lower left image screen of MetRec shows the segmented stars in the video stream. The lower right image shows the star map. All stars that are found in the segmented star image are highlighted. The left window informs that 175 out of 188 segmented stars were identified, which yields a limiting magnitude of +5.7.

2. from the pixel extent and the observing direction of the camera, the monitored surface (collection area) at the nominal meteor layer (100 km altitude) in square kilometers is obtained;

3. the loss in magnitude due to distance to the meteor layer (relative to 100 km) is calculated; and, finally,

4. the difference between the measured and the nominal limiting magnitude (+6.5) is transformed into a reduction of the effective collection area (assuming a population index of 3.0). That is, if the limiting magnitude is only +5.5, the measured collection area is reduced by a factor of 3.

In parallel to the limiting magnitude, also the effective observing time and the effective collection area are stored each minute.

To determine meteor shower flux densities, the effective collection area has to be specifically adjusted for each meteor shower, as follows:

1. the mean altitude of the meteor layer is calculated from the meteor shower velocity and radiant altitude (Molau and Sonotaco, 2008);

2. the average population index is taken from the IMO Meteor Shower Working List[1];

3. for each pixel, and additional loss in limiting magnitude due to the meteor motion is calculated. It is based on the integration time of the video camera and the expected apparent meteor velocity in degrees/second, which is transformed to pixels/frame; and, finally,

4. a correction factor for the radiant altitude is applied, as the number of meteors observable from a certain shower decreases the lower the radiant is located in the sky.

Each minute, MetRec stores for each shower the number of meteors and the effective collection area. The flux density is the number of shower meteors divided by the effective observing time and the shower-specific effective collection area. It represents how many meteoroids per hour capable of producing meteors brighter than magnitude +6.5 (in absolute brightness) are crossing an atmospheric layer of 1000×1000 km^2.

---

[1]http://www.imo.net/files/data/calendar/cal2013.pdf, Table 5, page 21.

3 MetRec Flux Viewer

There are two options to process the flux data obtained by METREC. After manual deletion of false detections, the updated flux density data can be uploaded off-line to the central Virtual Meteor Observatory (VMO) server. During particularly interesting nights, the data can be uploaded even in real-time (Molau et al., 2012a).

For the analysis, Geert Barentsen has implemented the METREC FLUX VIEWER[2]. It works similar to the visual data quicklook for visual observations[3], but it is analyzing and presenting the flux data uploaded by the IMO Video Meteor Network members. The web user can select a shower and then adjust the parameters of the flux display such as the time interval, the population, index or different binning criteria. The flux viewer creates a flux density plot from the available data, and optionally a data table.

The METREC FLUX VIEWER went live in April 2011, right in time for the Lyrids. It became a big success, as already this first trial led to a high-quality activity profile matching the visual quick look analysis quite well (Molau et al., 2011a). Even from the more cumbersome η-Aquariids (mainly observed at low altitudes) or α-Capricornids (with very low activity), we obtained remarkably accurate results. However, when it came to the 2011 Perseids, a supposedly simple case thanks to the large data set, we were surprised. The overall activity profile of the shower looked terrific, but the detailed profile of the maximum period was a disaster. The data chunks from the different nights did not fit to each other. Instead of presenting a smooth profile, the flux density grew continuously by more than a factor of 2 in some nights, even at the descending activity branch Figure 2.
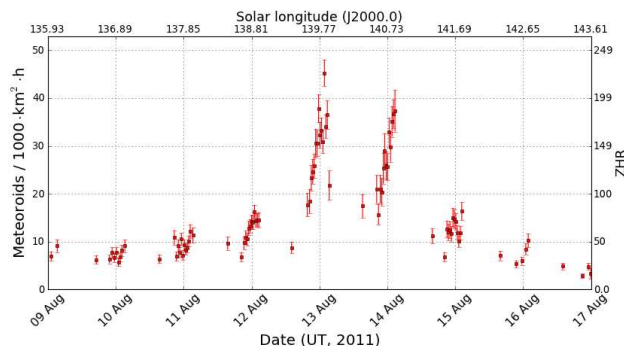

Figure 2 – Detailed flux density profile of the 2011 Perseids.

4 Radiant altitude correction function

After double-checking the calculation routine, it was obvious to assume that the odd behavior was linked to the radiant altitude, which was increasing from dusk till dawn as well. As described above, the radiant altitude is one important factor in the calculation of the

---

[2] http://vmo.imo.net/flx/.
[3] Cf. http://www.imo.net/live/orionids2012 for an example.

effective collection area. In the literature, different correction functions were discussed. A nice introduction is given by Richardson (1999).

The base form (Öpik, 1955) is a simple correction by the sine of the radiant altitude (or, equivalently, the cosine of the zenith distance), neglecting the curvature of Earth. Öpik had tried powers of the sine function higher than 1 before, but came to the conclusion that no zenith exponent was necessary. Kresák (1954) used the same function with an extra correction term for low altitudes (below 10°). Zvolánková (1983) revived the idea to raise the sine function to the power of some empirical correction factor γ, now dubbed the zenith exponent. From 17 000 visual Perseids, she obtained a value of $\gamma = 1.47$.

METREC combines the approaches of Kresák and Zvolánková, i.e., it uses the base function of Kresák, and raises it to the power of the zenith exponent. Since the correct zenith exponent is not known at this time and may depend on the meteor shower, a value of $\gamma = 1.0$ is applied by the software, and different values can later be set in the METREC FLUX VIEWER. For comparison, all correction functions are shown in Figure 3.

It should be noted that, for zenith exponents $\gamma > 1.0$, the expected meteor count is significantly lower compared to the plain sine correction. This is why flux densities (or ZHRs) which are calculated with a zenith exponent larger than one are higher than those obtained without a zenith exponent (Figure 4).

For the 2011 Perseids, we tested different values of γ and found empirically that $\gamma = 1.6$ reduces the variations best (Molau et al., 2011b). Later, we repeated the analysis for the 2011 Orionids and obtained a similar value of 1.5–1.6 (Molau et al., 2012a).

5 2012 Perseids

As the data set of the 2012 Perseids was particularly large, we decided to analyze the radiant altitude correction function in more detail. So far, most analyses where done by choosing a particular point in time (i.e., with fixed flux density), taking observers from different locations with different altitudes, and comparing their meteor count. Alternatively, the observations were first normalized to a mean ZHR profile.

To exploit the large size of our data set, we used a slightly different approach. First, we took the flux data from the VMO server and reverted the radiant altitude correction that was applied by MetRec. Then, we grouped the individual observing intervals of each camera by radiant altitude (with 5° bin size) and accumulated the uncorrected collection area and the meteor count for each radiant altitude bin. By dividing the meteor count by the collection area, we could calculate the average (uncorrected) flux density for each altitude bin. The data was normalized and finally averaged over all nights between August 1 and 21, 2012. The resulting
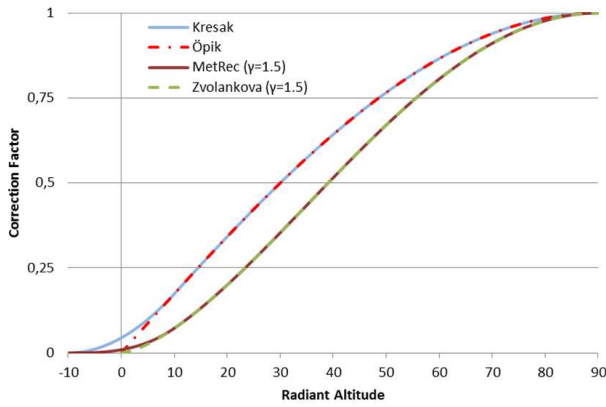
(a) General overview.
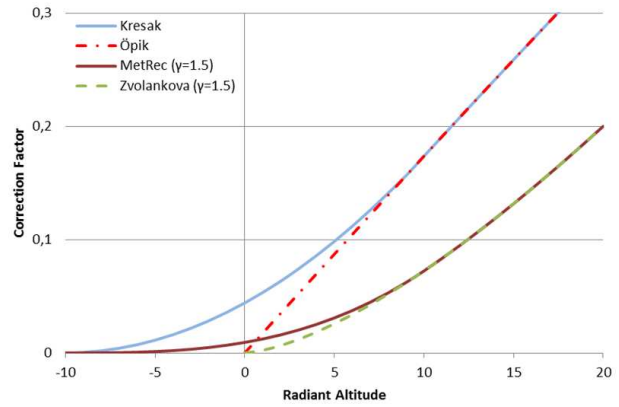
(b) Detail for low radiant altitudes.

Figure 3 – Radiant altitude correction function from different authors, and the function that is applied by METREC, with details for low radiant altitudes.
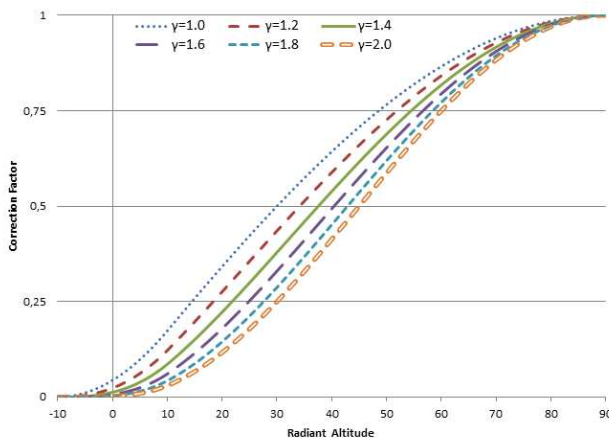

Figure 4 – Radiant altitude correction for different values of the zenith exponent γ.

flux density versus radiant altitude dependency is given in Figure 6, (a), calculated from 18 500 Perseids.

Our expectation was that, near maximum, nights during which the activity was strongly varying during the observation (e.g., low altitude bins at dusk would accumulate lower flux values than high altitude bins at dawn) should be omitted. That behavior was indeed observed in the plots of individual maximum nights, but it introduced no systematic deviation in the overall plot. The reason is probably that the inverse effect for ascending and descending branch nights cancelled out each other. Additionally, cameras at different locations at the same time contributed to different altitude bins. It also turned out that there was no need to normalize the activity of individual nights. The same dependency function was obtained by simple accumulation of collection area and meteor count for the same altitude bin over all Perseid nights. Even though the contribution of individual nights varied, the overall average graph was nearly the same.

Finally, a sine function with different zenith exponents was calculated and the value γ chosen which minimized the mean squared error to the measured dependency

function. It turned out that a zenith exponent of $\gamma = 1.9$ led to a very close match, as can be seen from Figure 6, (a). Applying that zenith exponent to the original data set improved the flux density graph significantly (Figure 5).

6   Further showers

We repeated the analysis for further meteor shower that we had recorded since April 2011 (Figure 6).

With 10 500 shower meteors, the 2011 Perseids gave a best match with $\gamma = 1.8$, i.e., almost the same value as for 2012. Also in this case, the estimate was quite reliable, as a large altitude range was covered.

For the analysis of the Southern δ-Aquariids, we combined 2011 and 2012 observation to obtain a data set of 4000 meteors. We only used European data in this case, because the data set from the southern hemisphere was too small and introduced systematic deviations. We obtained a zenith exponent of $\gamma = 1.75$, which is less reliable, though. If only a few low radiant altitude bins are available, different zenith exponents lead to only minor variations in the correction function.

The 2011 Orionid data set was large (11 000 meteors) and covered a sufficiently wide altitude range. Thus, the obtained zenith exponent of $\gamma = 1.55$ is reliable.

For the 2011 Leonids, we could not create a sensible plot because of data scarcity. Also, the Geminid plot based on 1500 meteors shows a lot of scatter, which is a pity, because the Geminids cover the largest altitude range and would be most valuable for this analysis. The best matching zenith exponent of $\gamma = 2.0$ must be interpreted with care.

The Taurids are a perfect shower for this type of analysis as well. They are active for two months, they show only little variation in activity, they present a wide range of radiant altitudes, and they provide an overall large data set. We combined Northern and Southern Taurids from 2011 and obtained a mean zenith expo-
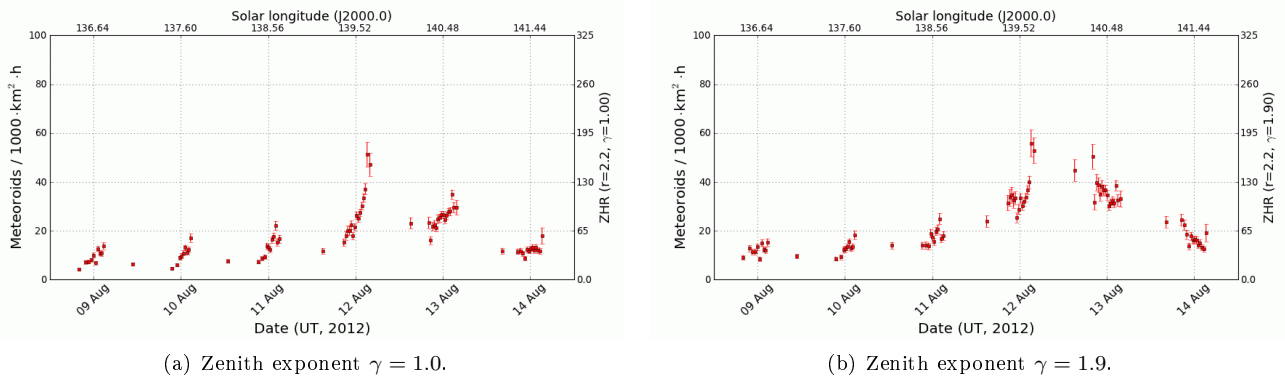
(a) Zenith exponent $\gamma = 1.0$.

(b) Zenith exponent $\gamma = 1.9$.

Figure 5 – Flux density profile of the Perseid 2012 with a zenith exponent $\gamma = 1.0$ (a) and $\gamma = 1.9$ (b).

Table 1 – Summary of the zenith exponent analysis results for individual meteor showers in 2011 and 2012. Unreliable results are printed in italic.

Shower	Year	Shower Meteors	Altitude range	Zenith exponent
Southern δ-Aquariids	*2011-12*	*4 000*	*0°–30°*	*1.75*
Perseids	2011	10 500	20°–65°	1.80
Orionids	2011	10 000	5°–55°	1.55
Taurids	2011	13 000	10°–65°	1.80
Geminids	*2011*	*1 500*	*5°–65°*	*2.00*
η-Aquariids	*2012*	*500*	*0°–25°*	*1.65*
Perseids	2012	18 500	20°–75°	1.90
Antihelion source	2011-12	8 300	0°–50°	1.65
Mean	2011-12	65 800	0°–75°	1.75

nent of $\gamma = 1.8$ from over 13 000 shower meteors. Even though the data set was large, there was still some noticeable scatter at large radiant altitudes.

From 500 η-Aquariids of 2012, we obtained a zenith exponent of $\gamma = 1.65$. Once again, this value is less reliable because of the small altitude range.

Last but not least, we determined the radiant altitude correction function for the Antihelion source, which is active all year long (except during the Taurids). Here, we cannot simply average over all nights, as systematic errors are introduced. Between November and March, when the radiant rises highest in the northern hemisphere, we observed a lower activity of the Antihelion source than in summer, when the radiant was low. So, the overall radiant altitude correction function deviated strongly from the normal shape. However, when we analyzed the intervals February–April and August–September separately with 8300 meteors overall, and then merged the data, the normal sine function with a zenith exponent of $\gamma = 1.65$ matched reasonably.

Table 1 summarizes the results for the individual showers. Figure 7, (a), combines all data sets in a single diagram, and shows also the mean values. This average graph can be modeled best by a sine function with a zenith exponent of 1.75, as shown in Figure 7, (b).

If we compare with previous work, Zvolánková, with $\gamma = 1.47$, found a result close to ours (Zvolánková, 1983). Much closer, however, is Schiaparelli's result; already back in 1871, he suggested a zenith exponent $\gamma = 1.6$ (Schiaparelli, 1871)!

It should be noted that this correction function is highly linear between the radiant altitudes of 15° and 75°. So, the radiant altitude correction could also be described by a linear function with a special correction term for altitudes below 15° (and probably above 75°, but that cannot be guaranteed from the existing data set, as these radiant altitudes were not sufficiently covered by our data).

7 Conclusions

We have shown that the dependency between the radiant altitude and the flux density can be well described by a sine function raised to the power of some zenith exponent γ.

Prerequisite for the accurate determination of the zenith exponent is that a large altitude range (of more than 45°) is covered. It is possible to combine data sets from different nights with different activity as long as the average flux density is approximately the same for all altitude bins.

We found strong indication in this study that the zenith exponent varies between different showers. The average value over all showers that we have analyzed so far is $\gamma = 1.75$.

Even when the right radiant altitude correction is applied, intervals with low radiant altitude should be omitted from flux density displays, since large correction factors will introduce large systematic errors.
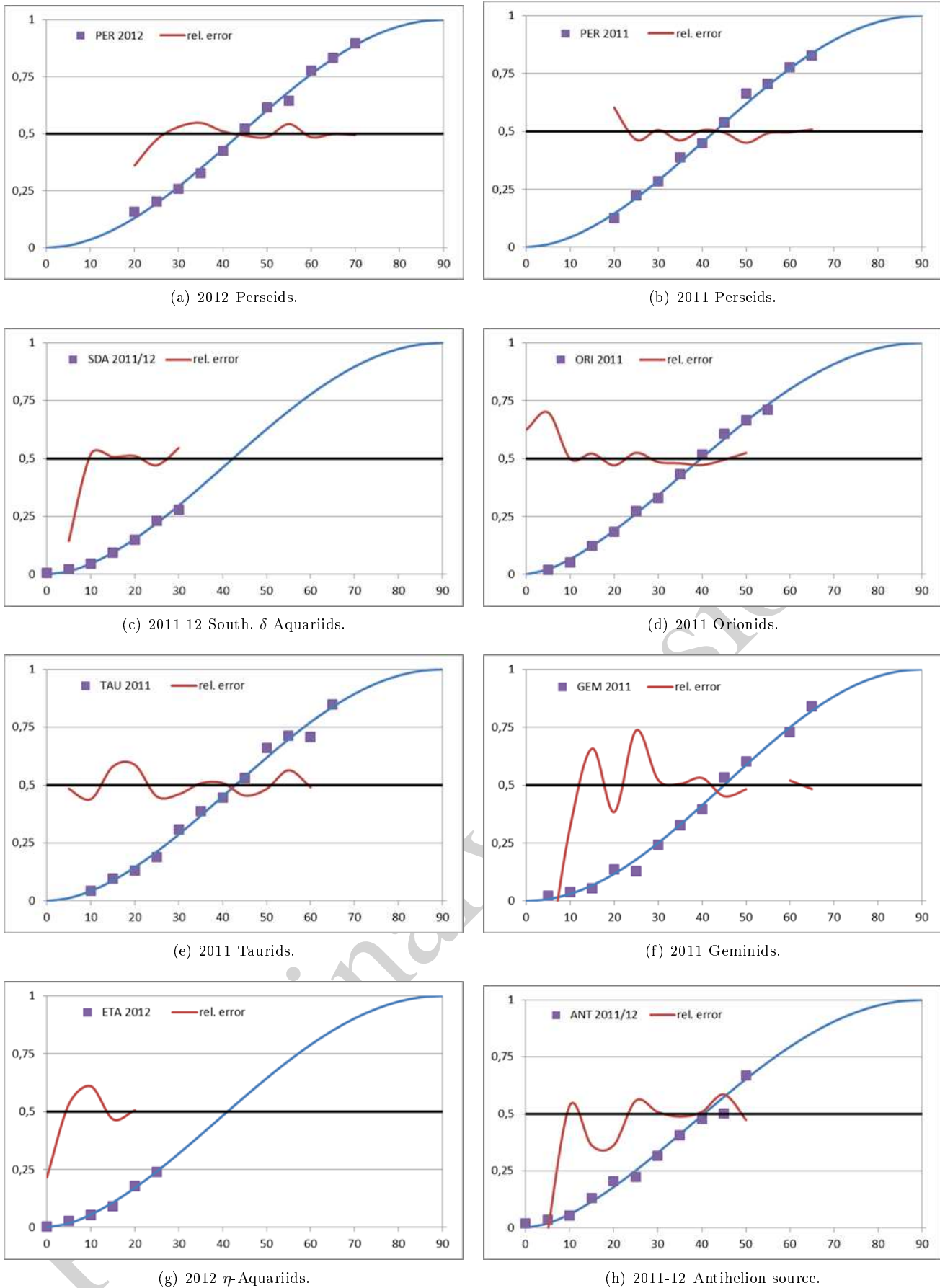
(a) 2012 Perseids.

(b) 2011 Perseids.

(c) 2011-12 South. δ-Aquariids.

(d) 2011 Orionids.

(e) 2011 Taurids.

(f) 2011 Geminids.

(g) 2012 η-Aquariids.

(h) 2011-12 Antihelion source.

Figure 6 – Radiant altitude correction function for different showers (a) 2012 Perseids; (b) 2011 Perseids; (c) 2011-12 Southern δ-Aquariids; (d) 2011 Orionids; (e) 2011 Taurids; (f) 2011 Geminids; (g) 2012 η-Aquariids; and (h) 2011-12 Antihelion source. Each graph shows the measured dependency (rectangles), the best correction function fit (blue line) and the relative deviation between the two (red line).
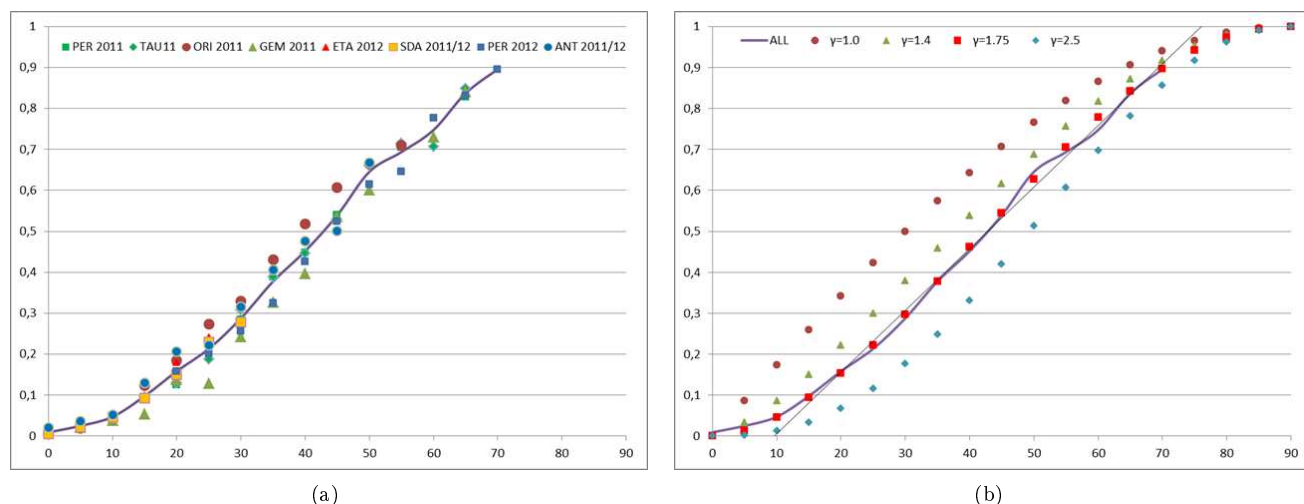
(a) (b)

Figure 7 – (a) Combination of the radiant altitude correction function from individual showers in 2011 and 2012 and their average. (b) The average correction function fits well to a sine function with a zenith exponent of $\gamma = 1.75$ (red rectangles), but can also be fitted by a linear function between 15° and 75° radiant altitude (black line).

Acknowledgements

References

Kresák L. (1954). "A nomogram for computing the zenith hourly rates of meteor showers" . *Bull. Astron. Inst. Czech.*, **6**, 220.

Molau S. (2010). "Towards flux rates from video meteor observations". Presented at the *International Meteor Conference*, Armagh, 16–19 September 2010, IMO.

Molau S., Kac J., Berko E., Crivello S., Stomeo E., Igaz A., and Barentsen G. (2011a). "Results of the IMO Video Meteor Network–April 2011". *WGN, Journal of the IMO*, **39**, 100–104.

Molau S., Kac J., Berko E., Crivello S., Stomeo E., Igaz A., and Barentsen G. (2011b). "Results of the IMO Video Meteor Network–August 2011". *WGN, Journal of the IMO*, **39**, 187–192.

Molau S., Kac J., Berko E., Crivello S., Stomeo E., Igaz A., and Barentsen G. (2011c). "Results of the IMO

Video Meteor Network–September 2011". *WGN, Journal of the IMO*, **39**, 193–198.

Molau S., Kac J., Berko E., Crivello S., Stomeo E., Igaz A., and Barentsen G. (2012a). "Results of the IMO Video Meteor Network—October 2011". *WGN, Journal of the IMO*, **40**, 41–47.

Molau S., Kac J., Berko E., Crivello S., Stomeo E., Igaz A., and Barentsen G. (2012b). "Results of the IMO Video Meteor Network—November 2011". *WGN, Journal of the IMO*, **40**, 48–52.

Molau S., Kac J., Berko E., Crivello S., Stomeo E., Igaz A., and Barentsen G. (2012c). "Results of the IMO Video Meteor Network—December 2011". *WGN, Journal of the IMO*, **40**, 69–75.

Molau S. and Sonotaco (2008). "On the average altitude of (video) meteors". *WGN, Journal of the IMO*, **36**, 124–130.

Öpik E. (1955). "The distriution of meteor stream intensity over the celestial sphere". *Contr. from Armagh Obs.*, **15**, 147–173.

Richardson J. (1999). "A Detailed analysis of the geometric shower radiant altitude correction factor" . *WGN, Journal of the IMO*, **27**, 308–317.

Schiaparelli G. V. (1871) *Entwurf einer astronomischen Theorie der Sternschnuppen.* Stettin, 1871.

Zvolánková J. (1983). "Dependence of the observed rate of meteors of the zenith distance of the radiant". *Bull. Astron. Inst. Czech.*, **34**, 122–128.